J Mater Sci (2007) 42:4508–4512
DOI 10.1007/s10853-006-0559-9

Mesocarbon microbeads supported PtSn catalysts for electrochemical oxidation of ethanol

Yuxia Bai · Jinfeng Li · Xinping Qiu ·
Jianjun Wu · Jianshe Wang · Jingyu Xi ·
Wentao Zhu · Liquan Chen

Received: 19 January 2006 / Accepted: 12 June 2006 /

Abstract Mesocarbon microbeads (MCMB) supported PtSn catalysts were prepared by alcohol reduction method and characterized by XRD, FESEM and EDX. XRD results show that the addition of Sn to Pt/MCMB extends the fcc lattice parameters of platinum and the particle size of PtSn/MCMB is about 2.6 nm, smaller than that of Pt/MCMB. The electrode catalytic activity in the electro-oxidation of ethanol was studied by cyclic voltammetry, Tafel plot, electrochemistry impedance spectra (EIS) and chronoamperometry. All the results showed that PtSn/MCMB gave higher catalytic activity for ethanol electro-oxidation than Pt/C (20 wt.% E-TEK).

Introduction

In recent years, direct alcohol fuel cell (DAFC) has been considered as one of the most promising power sources for transportation and portable electronic device [1–6]. However, the slow reaction kinetics of ethanol electro-oxidation is still the main obstacle for the application of direct ethanol fuel cell (DEFC). The complete oxidation of ethanol to CO_2 involves release of 12 electrons per ethanol molecule, C–C bond breaking and more adsorbed intermediate species that may poison the platinum catalysts, which make the reaction more complicated than that for methanol.

A lot of works focused on preparing the effective anodic catalyst with sufficiently high activity and CO-tolerance for ethanol electro-oxidation and found that Pt–Sn catalyst presents the high activity for the oxidation of ethanol [3, 7–10]. Xin and co-workers [7–9] prepared platinum-based catalyst by a polyol method and observed that addition of Sn, Ru and W improve the activity of Pt/C towards ethanol electro-oxidation in the order of $Pt_1Sn_1/C > Pt_1Ru_1/C > Pt_1W_1/C > Pt_1Pd_1/C > Pt/C$. They also investigated the effect of Sn content on the performance of DEFC and found that the Pt_3Sn_2/C is more suitable catalyst for the direct ethanol fuel cell at low temperature. Lamy et al. [3] also found that the modification of Pt by Sn improves the performance of DEFC. The maximum power obtained with Pt–Sn is three times the value found with Pt alone.

Usually the catalysts are formed in nanoparticles and dispersed on Vulcan 72 carbon black or other high surface area porous carbon to obtain optimum catalyst utilization. However, the carbon black, a kind of soft carbon material, may block the pores that are important for gas or liquid diffusion during the electrode reaction. So many researchers have conducted to use different kinds of carbon materials as support, such as ordered mesoporous carbon, carbon nanotubes (CNTs), hard carbon spherules (HCS) and mesocarbon microbeads (MCMB) [9, 11–15]. Recently Yang et al. [12] used HCS as support for Pt catalyst and obtained higher Pt utilization than that of the commercial catalyst Pt/C

Y. Bai · J. Li · X. Qiu (✉) · J. Wu · J. Wang ·
J. Xi · W. Zhu · L. Chen
Key Lab of Organic Optoelectronics and Molecular Engineering, Department of Chemistry, Tsinghua University, Beijing 100084, China
e-mail: qiuxp@mail.tsinghua.edu.cn

J. Wu
Department of Chemistry, Shijiazhuang College,
Shijiazhuang 050801, China

(E-TEK). It is believed that the special surface structure of HCS improved the capability of mass transport in the fuel cell.

Our previous work [13–15] demonstrated that MCMB are excellent candidates to be used as support for methanol electro-oxidation and are favorable for mass transport in fuel cell. Both of the catalysts of Pt/MCMB and PtRu/MCMB showed higher catalytic activity than commercial catalyst of Pt/C (E-TEK) for methanol electro-oxidation. Based on that, MCMB supported Pt–Sn catalyst was prepared by alcohol reduction method and their catalytic activity for ethanol electro-oxidation were evaluated by cyclic voltammetry, Tafel plot, electrochemistry impedance spectra (EIS) and chronoamperometry characterization techniques.

Experimental

Preparation and characterization of MCMB supported PtSn catalyst

MCMB supported PtSn catalyst (PtSn/MCMB) were prepared by reduction of H_2PtCl_6 and $SnCl_2$ precursor salts with ethylene glycol solution. Ethylene glycol was used as solvent and reducing reagent. First, 100 mg of MCMB was added to 30 mL of ethylene glycol and sonicated for 30 min in a 100 mL beaker. About 1 M KOH solutions were added dropwise up to a total volume of 2 mL. When the temperature was increased up to 120 °C, the mixture of H_2PtCl_6 and $SnCl_2$ solution was added under stirring and the temperature was kept constant in oil bath for 2 h. Then the resultant sample was filtered and washed with deionized water and ethanol repeatedly. Finally the product was dried at 70 °C in vacuum for 12 h. The Pt/MCMB was also prepared by the same procedures as PtSn/MCMB.

The surface morphologies and the composition of the PtSn/MCMB catalyst were examined by a thermal field emission scanning electron microscope (SEM LEO1530) equipped with energy-dispersive X-ray spectroscopy (EDX). And the X-ray diffraction (XRD) patterns of all samples were obtained with a Rigaku X-ray diffractometer using CuKα radiation source. The 2θ angular regions between 20° and 90° were explored at a scan rate of 6° min^{-1} with step of 0.02°

Preparation and characterization of electrodes

The catalyst ink was prepared by mixing the catalyst with perfluorsulfonic acid solution (5 wt.%, Nafion®, Du Pont), ethylene glycol, water and acetylene black (10 wt.%) ultrasonically. Then the slurry was spread on a gold foil of ca. 1.6 cm^2. Then the electrode was dried at 80 °C for 2 h. The total catalyst loadings were about 0.5 mg/cm^2.

Electrochemical measurements were carried out using a Solartron 1287 electrochemical interface and 1255B frequency response analyzer in a three electrode cell at 25 °C. The gold foil coated with catalyst ink was used as working electrode. Before used, the gold electrode was polished and rinsed ultrasonically in deionized water. A saturated calomel electrode (SCE) and Pt foil were used as reference and counter electrodes, respectively. All electrode potentials in this paper were referred to the SCE. A solution of 1.0 M $HClO_4$ + 1.0 M ethanol was used as electrolyte. All the reagents used were of analytical grade. The cyclic voltammetry data were recorded in the potential range of –0.2 to 1 V versus SCE with a scan rate of 50 mV/s. Electrochemical impendence spectra (EIS) was performed with amplitude of 10 mV in the frequency range 10^6–0.1 Hz at 0.4 V versus SCE.

Results and discussion

Figure 1 shows the SEM imagines of PtSn/MCMB. As shown in Fig. 1a, MCMB particles, with an average particle size of 10–12 μm, have a spherical shape, consisting of many small graphite crystals. The surface of MCMB particles is not smooth and has many nodular lumps and pores, which are helpful for the adsorption of catalyst particles [14]. After reduction in ethylene glycol, PtSn nanoparticles homogeneously disperse on the surface of the MCMB, which can be seen more clearly in Fig. 1b. EDX analysis confirmed the presence of Pt and Sn and the Pt:Sn atomic ratios of the obtained PtSn/MCMB were 1.16:1.19.

XRD patterns of Pt/MCMB and PtSn/MCMB are shown in Fig. 2. The peaks marked with asterisks are attributed to graphitic MCMB (100), (101) and (004). For Pt/MCMB the diffraction peaks at about 39°, 46°, 68° and 81° are observed, corresponding to Pt (111), (200), (220) and (311) plane, respectively. While for PtSn/MCMB, the diffraction peaks of Pt turn broader and only Pt (111) diffraction peaks at about 39° can be clearly recognized, which had been observed in the XRD patterns of carbon supported PtSn [16]. The broader diffraction peaks may be related with the smaller Pt nanoparticle size. The average particle size is 2.6 nm for PtSn/MCMB estimated from Pt (111) by the Scherrer formula [17], smaller than that for Pt/MCMB (3.95 nm). And for PtSn/MCMB, the diffraction peak of Pt (111) shift to lower position compared

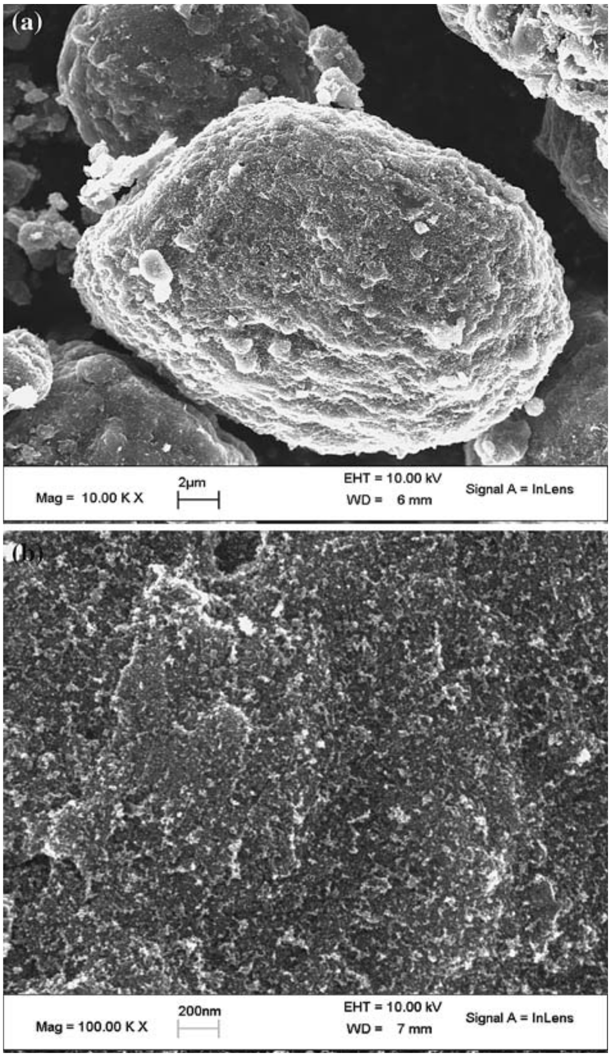

Fig. 1 (**a**) SEM image of PtSn/MCMB catalyst. (**b**) The dispersion of PtSn on MCMB support

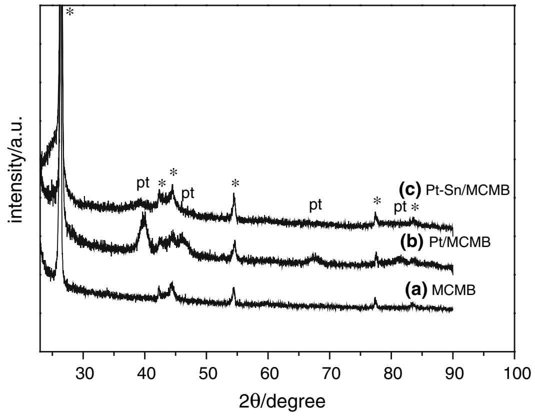

Fig. 2 XRD patterns of (a) bare MCMB powders, (b) Pt/MCMB, (c) PtSn/MCMB

with that for Pt/MCMB, which is similar to that for carbon supported PtSn [16]. The lattice parameter of PtSn/MCMB is estimated to be 3.980 Å, and the lattice parameter of Pt/MCMB is 3.924 Å, indicating the incorporation between Pt and Sn.

The representative voltammogram curve for ethanol electro-oxidation on PtSn/MCMB is presented in Fig. 3. The scan rate was 50 mV/s in the range –0.2 to 1 V versus SCE. The CV curve for ethanol electro-oxidation on Pt/C (20 wt.% Pt, E-TEK) is also presented in Fig. 3 to compare the activity of Pt/C with that of PtSn/MCMB. As expected, in the presence of Sn the onset potential for the ethanol electro-oxidation is shifted to lower potential with respect to Pt/C. The forward scan peak potential of the ethanol electro-oxidation locates at 0.86 V versus SCE for Pt/C electrode and the peak potential negatively shifts to 0.77 V for PtSn/MCMB. PtSn/MCMB has higher peak current density in comparison with Pt/C. The results show that PtSn/MCMB has higher catalytic activities for ethanol oxidation than Pt/C. The high electrocatalytic activity of the PtSn/MCMB catalyst may be related with the high dispersion of the PtSn nanoparticles on MCMB support, and the improved capability of mass transport of ethanol in the electrode [13]. Except that, the Sn addition favors the low potential oxidation of adsorbed intermediate species such as CO and CO-like intermediates, which promote the electrocatalytic activity of platinum to alcohol electro-oxidation. [18, 19].

Figure 4 shows the polarization curves of PtSn/MCMB and Pt/C catalyst. The ethanol oxidation currents were obtained from current–time transient values recorded at a particular potential for several minutes. As shown in Fig. 4, PtSn/MCMB displays the lower overpotential than Pt/C.

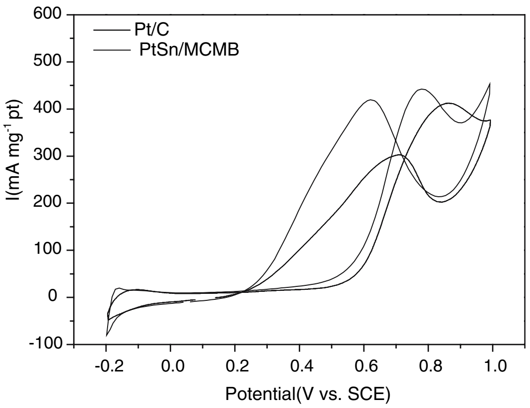

Fig. 3 Cyclic Voltammogram curves of the Pt/C and PtSn/MCMB electrode in 1 M $HClO_4$ + 1 M C_2H_5OH solutions at scan rate of 50 mV/s

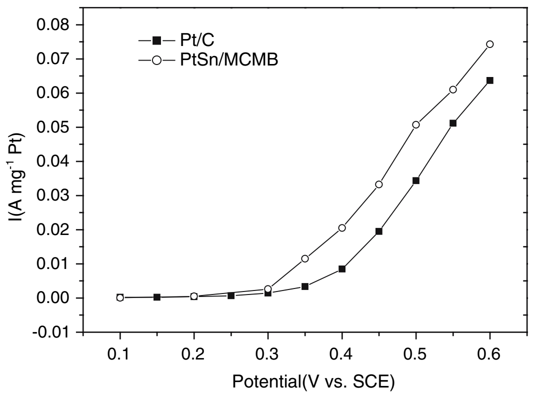

Fig. 4 Polarization curves for the electro-oxidation of ethanol in 1 M $HClO_4$ + 1 M C_2H_5OH on Pt/C and PtSn/MCMB electrode

Nyquist plots of the impedance for ethanol electro-oxidation on PtSn/MCMB and Pt/C catalyst at potential of 0.4 V versus SCE were summarized in Fig. 5. The simplified equivalent circuit shown in Fig. 5 was used to fit the EIS data. Here Rs is the solution resistance. Rct is the charge transfer resistance at the interface of the catalyst layer. A constant phase element (CPE) is an electrical component to model the double layer capacitance at metal–solution interface. The double layer capacitance was found to be 0.020 and 0.045 F for PtSn/MCMB and Pt/C, respectively. And the charge transfer resistance was found to be 42.2 Ω for PtSn/MCMB and 62.67 Ω for Pt/C. It is known that the magnitude of Rct is related with the resistance involved in ethanol electro-oxidation kinetic. The smaller Rct value means that PtSn/MCMB has the higher catalytic activity for ethanol electro-oxidation.

The chronoamperometric measurements were carried out in 1 M $HClO_4$ + 1 M C_2H_5OH solution at potential of 0.4 V for 1,800 s, aiming at verifying the catalytic activities of PtSn/MCMB electrode under constant potential. Pt/C electrode was also included in this measurement for comparison. It is seen from Fig. 6 that there is an initial current drop and reach stable within 400 s on both of PtSn/MCMB and Pt/C electrode. PtSn/MCMB electrode shows a higher current value of 7.11 mA mg^{-1} after 1,800 s of electrolysis, whereas the electrode Pt/C presents the current value of 4.34 mA mg^{-1} indicating that PtSn/MCMB has higher activity than Pt/C.

Conclusion

In this work, we prepared MCMB supported PtSn catalyst by alcohol reduction process. The X-ray diffractograms of Pt/MCMB and PtSn/MCMB show the typical fcc structure of platinum and the average particle size is 3.95 and 2.6 nm for Pt/MCMB and PtSn/MCMB, respectively. The addition of Sn to Pt/MCMB extends the fcc lattice parameters of platinum indicating the interaction between Pt and Sn. The PtSn/MCMB presents lower peak potential and higher current density toward ethanol electro-oxidation compared with Pt/C. The result of polarization curve shows that PtSn/MCMB has lower overpotential for ethanol electro-oxidation. The charge transfer resistance of PtSn/MCMB is also smaller than Pt/C as found in the impedance spectra, indicating an increase in reaction kinetics.

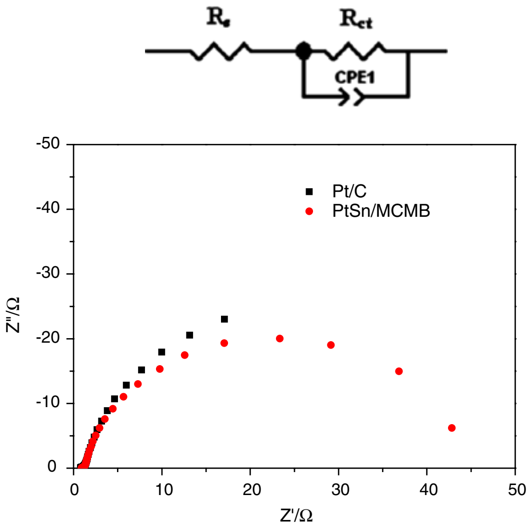

Fig. 5 Nyquist plots of EIS for ethanol electro-oxidation on Pt/C and PtSn/MCMB electrodes in 1 M $HClO_4$ + 1 M C_2H_5OH solutions at 0.4 V versus SCE and corresponding equivalent circuits

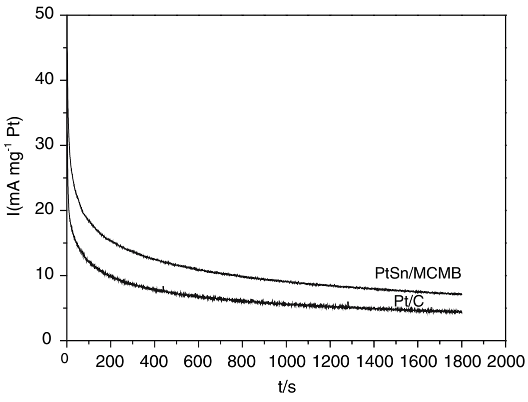

Fig. 6 Chronoamperometric responses during ethanol electro-oxidation on Pt/C and PtSn/MCMB electrode in 1 M $HClO_4$ + 1 M C_2H_5OH solutions at the potential of 0.4 V versus SCE

Acknowledgements The authors appreciate the financial support of the State Key Basic Research Program of PRC (2002CB211803) and National Natural Science Foundation of China (90410002).

References

1. Chen CY, Yang P (2003) J Power Sources 123:37
2. Vigier F, Coutanceau C, Perrard A, Belgsir EM, Lamy C (2004) J Appl Electrochem 34:439
3. Lamy C, Rousseau S, Belgsir EM, Coutanceau C, Léger J-M (2004) Electrochim Acta 49:3901
4. Spinace EV, Neto AO, Linardi M (2004) J Power Sources 129:121
5. Jiang LH, Zhou ZH, Li WZ, Zhou WJ, Song SQ, Li HQ, Sun GQ, Xin Q (2004) Energy Fuels 18:866
6. Wang H, Jusys Z, Behm RJ (2004) J Phys Chem B 108:19413
7. Zhou WJ, Zhou ZH, Song SQ, Li WZ, Sun GQ, Tsiakaras P, Xin Q (2003) Appl Catal B: Environ 46:273
8. Jiang LH, Sun GQ, Zhou ZH, Zhou WJ, Xin Q (2004) Catal Today 93–95:665
9. Zhao XS, Li WZ, Jiang LH, Zhou WJ, Xin Q, Yi BL, Sun GQ (2004) Carbon 42:3251
10. Antolini E, Cardeilini F, Giorgi L (2000) J Mater Sci Lett 19:2099
11. Ding J, Chana KY, Ren JW, Xiao FS (2005) Electrochim Acta 50:3131
12. Yang RZ, Qiu XP, Zhang HR, Li JQ, Zhu WT, Wang ZHX, Huang XJ, Chen LQ (2005) Carbon 43:11
13. Liu YC, Qiu XP, Huang YQ, Zhu WT (2002) Carbon 40:2375
14. Liu YC, Qiu XP, Huang YQ, Zhu WT (2002) J Power Sources 111:160
15. Liu YC, Qiu XP, Huang YQ, Zhu WT, Wu GS (2002) J Appl Electrochem 32:1279
16. Jiang LH, Zang HX, Sun GQ, Xin Q (2006) Chinese J Catal 27:15
17. Radmilovic V, Gasteiger HA, Ross PN Jr (1995) J Catal 154:98
18. Zhou WJ, Zhou B, Li WZ, Zhou ZH, Song SQ, Sun GQ, Xin Q, Douvartzides S, Goul M, Tsiakaras P (2004) J Power Sources 127:16
19. Abdel Rahim MA, Khalil MW, Hassan HB (2000) J Appl Electrochem 30:1151